



**HAL**  
open science

## Silicon etching in a pulsed HBr/O<sub>2</sub> plasma. I. Ion flux and energy analysis

Moritz Haass, Maxime Darnon, Gilles Cunge, Olivier Joubert, David Gahan

### ► To cite this version:

Moritz Haass, Maxime Darnon, Gilles Cunge, Olivier Joubert, David Gahan. Silicon etching in a pulsed HBr/O<sub>2</sub> plasma. I. Ion flux and energy analysis. *Journal of Vacuum Science and Technology*, 2015, 33 (3), pp.032202. 10.1116/1.4917230 . hal-01878009

**HAL Id: hal-01878009**

**<https://hal.univ-grenoble-alpes.fr/hal-01878009>**

Submitted on 1 Sep 2020

**HAL** is a multi-disciplinary open access archive for the deposit and dissemination of scientific research documents, whether they are published or not. The documents may come from teaching and research institutions in France or abroad, or from public or private research centers.

L'archive ouverte pluridisciplinaire **HAL**, est destinée au dépôt et à la diffusion de documents scientifiques de niveau recherche, publiés ou non, émanant des établissements d'enseignement et de recherche français ou étrangers, des laboratoires publics ou privés.



Distributed under a Creative Commons Attribution 4.0 International License

# Silicon etching in a pulsed HBr/O<sub>2</sub> plasma. I. Ion flux and energy analysis

Moritz Haass, Maxime Darnon,<sup>a)</sup> Gilles Cunge, and Olivier Joubert

LTM (CNRS/UJF-Grenoble1/CEA), 17 Avenue des Martyrs, 38054 Grenoble Cedex 9, France

David Gahan

Impedans Ltd., Unit 8 Woodford Court, Woodford Business Park, Santry, Dublin 17, Ireland

(Received 29 September 2014; accepted 17 March 2015; published 9 April 2015)

The ion flux and ion velocity distribution function are studied using a capacitively coupled radio frequency ion flux probe and a multigrid retarding field analyzer in an HBr/O<sub>2</sub> pulsed plasma process, dedicated to silicon etching in gate or shallow trench isolation applications. A decrease of the duty cycle of the pulsed plasma etch process affects strongly these parameters: the mean ion flux decreases almost by the square of the duty cycle. Furthermore, the contribution of high energy ions from the on-time of the plasma is strongly reduced while their energy is slightly increased. In average, this leads to a significantly reduced ion energy and a reduced ion flux in the pulsed plasma compared to the continuous wave plasma. © 2015 American Vacuum Society.

[<http://dx.doi.org/10.1116/1.4917230>]

## I. INTRODUCTION

The continuous downscaling of microelectronic devices imposes increasing demands on the plasma processes in terms of etch homogeneity, profile tolerance, surface damage, etch materials, throughput and reproducibility. Especially the plasma-induced damage becomes difficult to control since the tolerance range for deformations and surface alterations decreases permanently. Currently, the traditional ways for process optimization to meet the increasing demands reach their limits. New strategies to overcome these limiting factors are needed and innovative approaches are being developed. One of these is the use of pulsed high-density plasmas. In this case, the RF for inductively coupled plasma (ICP) plasma generation and the optional additional RF for ion acceleration (biasing of the substrate) are pulsed in various modes: synchronously (source and bias) at various frequencies with adjustable phase lags and duty cycles, or independently, e.g., with one generator in continuous wave (CW) mode.

Several authors reported process improvements due to decreased charging effects,<sup>1-6</sup> reduced surface damage,<sup>7,8</sup> lower ion energies,<sup>6,9,10</sup> reduced UV flux,<sup>11,12</sup> increased plasma uniformity,<sup>13,14</sup> and an improved selectivity.<sup>10,15</sup>

Although explanations for the individual observations have been proposed, a complete picture of the fundamental processes that lead to the observed results is still missing. The knowledge of the impact of the plasma pulsing parameters on the plasma chemistry and ion flux and energy is indispensable to fully identify the potential of pulsed plasmas and to transfer the already published results to other plasma chemistries and applications.

In a series of two articles, we investigate the impact of plasma pulsing on an HBr/O<sub>2</sub> silicon etch process, dedicated to gate, fin or shallow trench etching.

In this paper, the ion flux and energy is studied by using two different probes. The first one is a capacitively coupled RF probe<sup>16,17</sup> that measures the ion flux at the reactor walls.

The advantage of this kind of probe is that it is almost unaffected by deposited layers on its surface. The second probe is a retarding field analyzer (RFA)<sup>18,19</sup> that gives information on the ion flux and the ion velocity distribution function (IVDF). The focus of the experiments lies on the impact of the pulse parameters.

In Paper II,<sup>20</sup> the presented results are used to explain the strong impact of plasma pulsing on actual pattern transfer.

Although HBr/O<sub>2</sub> plasmas are commonly used in the semiconductor industry, their composition has hardly been studied. Pargon *et al.*<sup>21</sup> investigated the ion composition by mass spectrometry for an HBr/O<sub>2</sub> (70/30 sccm) plasma and found that H<sub>3</sub>O<sup>+</sup> was the most common ion that was detected. Cunge *et al.*<sup>22</sup> studied the ion flux composition of HBr/O<sub>2</sub>/Cl<sub>2</sub> plasmas. However, due to the additional Cl<sub>2</sub>, it is difficult to derive results for a pure HBr/O<sub>2</sub> plasma. Furthermore, the impact of plasma pulsing on HBr plasmas (without O<sub>2</sub>) has been studied, showing that the duty cycle controls the plasma chemistry: as the duty cycle is reduced the densities of molecular species (HBr, Br<sub>2</sub>) rise while the density of atomic radicals (Br) drops.<sup>23</sup> To our knowledge, the neutral composition of an HBr/O<sub>2</sub> plasma has not been studied in detail yet.

## II. EXPERIMENTAL SETUP

In this paper, we investigate HBr and HBr/O<sub>2</sub> plasmas used for silicon etching in continuous wave and pulsed conditions. A baseline process with 200 sccm HBr, 750 W of source power, and a pressure of 20 mT is chosen. This corresponds to typical process conditions for silicon etching in the semiconductor industry. For the analysis of HBr/O<sub>2</sub> plasma, 5 sccm of O<sub>2</sub> is added. When silicon is etched, an additional 200 W of bias power are used. In pulsed conditions, both source and bias power supplies are pulsed simultaneously. Standard condition is 1 kHz for the pulsing frequency while the duty cycles varies between 10% and 75%.

In the first part of the paper, we analyze the ion flux without bias power in CW plasma or in pulsed conditions with a pulsing frequency of 1 kHz and a duty cycle varying between

<sup>a)</sup>Electronic mail: Maxime.Damon@USherbrooke.ca

10% and 75%. Then, we analyze the impact of the bias power on the ion flux and energy in continuous wave plasmas. Ion flux and ion energy are then analyzed in pulsed plasma for a constant pulsing frequency of 1 kHz and various duty cycles, and with constant duty cycles of 20%, 50%, or 75% and changing frequencies. For ion energy analysis in pulsed plasmas, the plasma conditions were modified to maximize the signal to noise ratio and limit the ion energy to less than 400 eV (maximum energy acceptable by our RFA system), i.e., the source power was increased to 1200 W, the pressure decreased to 10 mTorr, and the bias power was limited to 60 W.

The experiments are conducted in a commercially available 300 mm AdvantEdge™ DPS etch tool from Applied Materials, Inc. The plasma is sustained by two ICP coils (source), powered at 13.56 MHz, while the chuck is biased via a capacitively coupled RF power source (bias), likewise working at 13.56 MHz. The power supply is modified with the Pulsync™ system to allow pulsing of the source and bias power with frequencies between 100 and 20 kHz and duty cycles between 10% and 90%. More details about the etch reactor can be found in the literature.<sup>24</sup>

### A. Ion flux probe

The ion flux is a crucial parameter for etching processes. In this study, a planar ion flux probe (IFP), developed by Braithwaite *et al.*<sup>16</sup> and Booth *et al.*<sup>17</sup> and recently adapted to pulsed plasma measurements,<sup>25</sup> was used to directly measure the ion flux onto its surface. The probe itself consists of a large area (1 cm<sup>2</sup>) planar single-sided disk, which is positioned in plane to the plasma reactor wall about 5 cm above the wafer support. A guard ring with the same surface is placed around the probe to avoid edge effects of the sheath (see Fig. 1).

A pulsed RF source is coupled to the probe and the guard ring via capacitors. Thanks to this blocking capacitor  $C_b$ , a dc self bias ( $V_{\text{bias}}$ ) can develop on the probe surface when it is fed with RF power. This effect is equivalent to the self-bias effect of the powered electrode in a capacitively coupled plasma.

After the RF voltage is turned off, the accumulated charge on the plasma side of the capacitor remains. If  $V_{\text{bias}}$  is

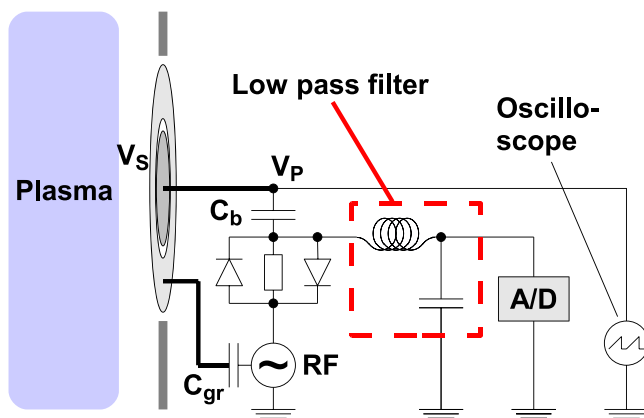


FIG. 1. (Color online) Sketch of the ion flux probe with direct current measurement.

sufficiently negative with respect to the plasma potential (several 10 V), the electron flux  $\Gamma_e$  will be negligible compared to the ion flux  $\Gamma_i$  on the probe surface and the blocking capacitor is therefore going to discharge by collecting the ion Bohm flux from the plasma.

The ion induced current is measured directly over a resistor that is placed in parallel with two head-to-tail diodes in between the blocking capacitor and the RF generator. The potential drop is measured with a high resolution analog-digital converter from National Instruments at a sample rate of 1.2 MHz with a maximum voltage input of 10 V.

When the probe pulsed RF power supply is correctly synchronized with the pulsed plasma RF power supply, this technique can be used to study pulsed plasma discharges.<sup>25,26</sup> In this case, the time during which the probe discharges needs to be at least as long as one entire period of the plasma RF pulse. The full details on the application of the planar probe for pulsed plasmas analysis are explained elsewhere.<sup>25</sup>

The error bar for the ion flux measurement is considered to be below 5%. This mostly comes from nonperfect edge effect suppression by the guard ring and RF noise in the measurement system. Additional errors from the electronic circuit may lead to systematic errors of a few percent. However, these errors do not change the relative variations observed on the measurement and are not included in the error bars.

### B. Retarding field analyzer

An alternative diagnostic tool to measure the ion flux, but in addition the IVDF, is a RFA. In this article, several prototypes of the commercially available SEMION probe from Impedans, Ltd., were used.<sup>18,19</sup> In Fig. 2(a), the schematic of such a four grid analyzer is shown.

The first grid  $G_1$  is a floating grid to simulate the potential of the floating wall or the wafer. If the RFA is positioned on a biased wafer, the self-bias potential is transmitted via the metallic frame to  $G_1$ . The second grid  $G_2$ , called the discriminator grid, is biased with a potential ramp to discriminate the ion energy. The third grid  $G_3$  functions as a suppression grid to repel electrons from the plasma and to prevent secondary electrons from the ion bombardment of the collector to escape. The fourth grid (or plate) C is the collector. The current from the incoming ion flux is measured at each step of the potential ramp.

All grids are connected via high impedance low-pass filters to an external power supply, which is controlled via Universal Serial Bus by a Personal Computer. The floating potential of  $G_1$  is measured externally with an oscilloscope with respect to an external ground. While all grids follow the RF component of the plasma power supply and the consequential potential changes of this time scale, only  $G_1$  follows also the averaged DC bias/floating potential of the substrate due to its direct electrical connection. This means that the incoming ions “see” a surface with floating potential ( $G_1$ ). The nonfloating grid potentials at  $G_2$ ,  $G_3$ , and C are set with respect to the external ground. Hence, the floating voltage

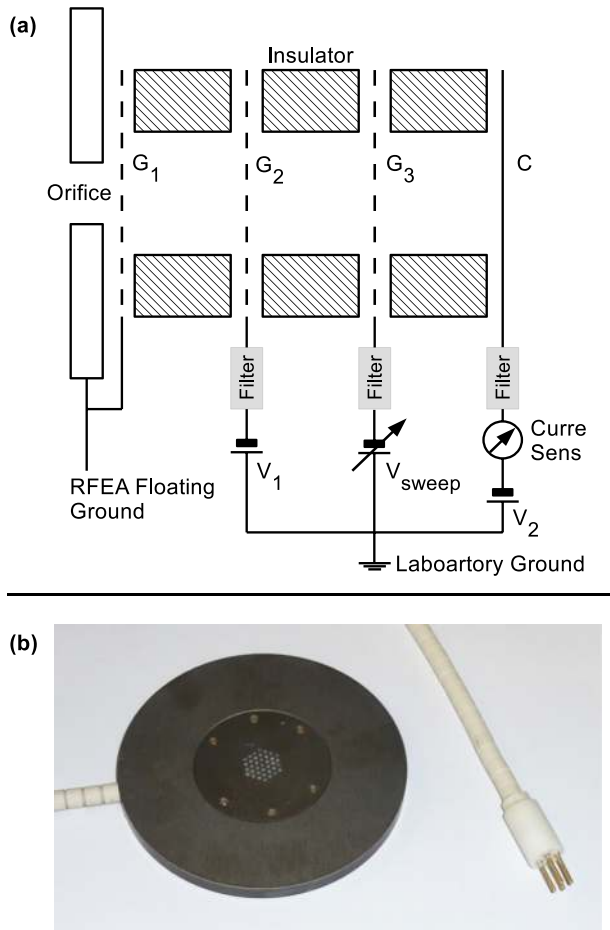


FIG. 2. (Color online) (a) Example of an RFA with four grids<sup>18</sup> and (b) a photo of the used probe with anodized aluminum cover.

from  $G_1$  needs to be subtracted from the discriminator voltage values to obtain the ion energy with respect to the floating surface. Under these conditions, the measured current–voltage (I–V) data from C (collector current) and  $G_2$  (varied discriminator voltage) represents the total flux of ions and can be differentiated to obtain the IVDF.

For all experiments presented later, the RFA was placed in the center of a 300 mm diameter silicon wafer. For the first two measurement sessions, a thin ceramic shield ( $\sim 2$  mm) with 0.8 mm holes for ion collection was used to prevent the metallic body of the sensor from etching. In a third session, the aluminum body itself was anodized (same material as reactor walls) and thereby converted to a dielectric shield. Only measurements with the same setup are compared since the transmission function might change between different hardware designs.

Two examples of the measured I–V curve and the resulting IVDF are shown in Fig. 3. Under plasma conditions where the ion current is large, the IVDF can be obtained by direct derivation of the I–V characteristic, as shown in Fig. 3(a). However, in some cases (typically in pulsed plasmas at low duty cycle), the I–V measurement is very noisy, so that no information can be obtained from the derivative (IVDF). In this case, the I–V curve can be fitted with a combination of several logistic (Boltzmann) functions and, if necessary, with an additional linear term accounting for the escaping

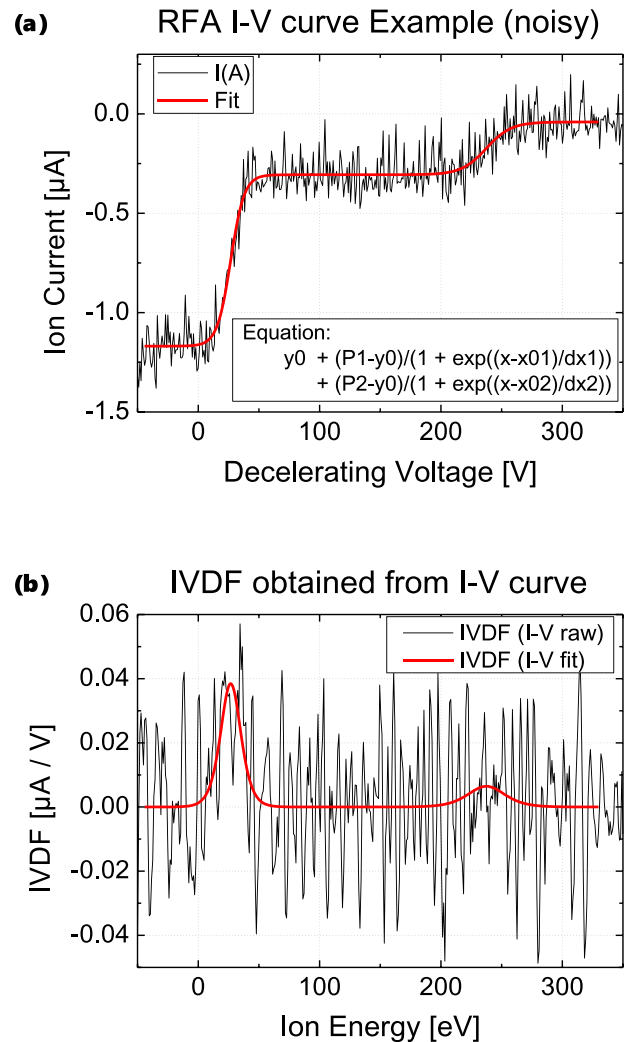


FIG. 3. (Color online) (a) Measured I–V curve of the RFA with fit. (b) Direct derivative (IVDF) of raw data and derivative of fit.

secondary electrons in order to obtain a smooth IVDF. From this fit function a derivative can be obtained.

Regarding the error of the RFA measurements, two errors need to be distinguished. One is the error of the absolute energy and the other is the error of the ion flux at that energy. Considering the RFA geometry and the electronics, the energy measurement error is considered to be less than 10%. For the ion flux, only ions are measured that arrive at the collector and it is difficult to calculate the original flux arriving at the RFA outer surface, especially if the design changes between experiments. Therefore, only the relative ion flux evolution and its error of less than 5% are shown. The error mainly results from geometric effects and temperature variations.

### III. ION FLUX WITHOUT BIAS

#### A. Necessity of reactor coating for reproducible results

Since the IFP is unaffected by a thin deposited layer on its surface, it is well suited to investigate the influence of different reactor wall surface conditions on the ion flux. Indeed, it is well known that the chemical nature of the reactor has a

strong impact on the plasma chemistry in halogen-based plasmas.<sup>27–30</sup> Therefore, the ion flux was investigated for CW HBr and HBr/O<sub>2</sub> plasmas at 20 mTorr and 750 W source power that are operated either in “seasoned” chamber (SiO<sub>2</sub> coating formed on reactor walls prior to etch process) or in “clean walls” reactor conditions (exposure to an SF<sub>6</sub>/O<sub>2</sub> plasma prior to etch process). During the actual etch conditions, a layer consisting of Si, Br, O, and H is deposited on the reactor wall.

Figure 4 shows the obtained ion fluxes in clean and seasoned condition. Significant differences of the ion flux can be observed.

The ion flux results from the ionization of neutral species upon electron impact in the plasma. It is therefore highly dependent on the electron density, the electron temperature, and the density and the ionization cross section of each neutral species. On the other hand, the neutrals’ composition is strongly dependent on the recombination and sticking coefficient of the neutral species at the chamber walls. Therefore, changes in the chamber wall conditions result in changes in the neutrals’ composition and consequently changes in the ion flux. For our specific conditions, our data indicate that the ion flux is larger for the HBr plasma in seasoned conditions than in cleaned conditions, while it is vice versa for the HBr/O<sub>2</sub> plasma. This tends to indicate that the density of neutral species with a high ionization cross section is larger in seasoned conditions than in clean conditions for the HBr plasma while it is the contrary for HBr/O<sub>2</sub> plasma. Oxygen containing ions such as H<sub>3</sub>O<sup>+</sup> are probably involved in the differences. The exact source for the difference between both plasma conditions is not fully explained here and would require a complete chemical analysis of the plasma species, which is out of the scope of this paper. These data illustrate though the necessity of controlled chamber wall conditions prior to the experiments to ensure reproducible results. Working in seasoned chamber conditions is preferable since it prevents a significant variation of the ion flux along the process that would result from the progressive coating of the chamber walls by SiO<sub>x</sub> species.

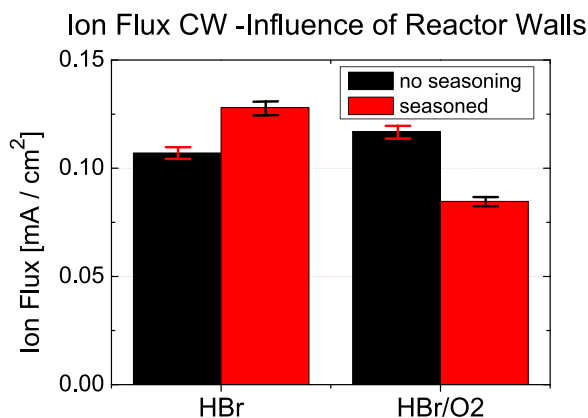


FIG. 4. (Color online) Influence of the nature of the reactor walls on the ion flux in an HBr and an HBr/O<sub>2</sub> CW plasma at 20 mTorr and 750 W source power. The seasoning consists of a thin layer of SiO<sub>2</sub> on the walls compared to a “clean” chamber where deposited layers have been removed by an SF<sub>6</sub>/O<sub>2</sub> plasma.

## B. Ion flux in pulsed plasmas

In Fig. 5, the measured ion flux in an HBr and in an HBr/O<sub>2</sub> plasma at 20 mTorr and 750 W source power is shown for different duty cycles at a frequency of 1 kHz.

For all pulsed cases, the ion flux increases continuously during the on-time of the source power and never reaches a steady state as it is the case for a CW plasma.

While in the pure HBr plasma, the ion flux rises strongly at first and then slows down, the ion flux in the HBr/O<sub>2</sub> plasma starts out with a slow increase that accelerates later during the on-time of the pulse. The slow decrease in the afterglow on the other hand is comparable in both chemistries.

Interestingly, both plasmas show an additional fast variation of the ion flux when the power is switched on or off. This is attributed to a fast change of the electron temperature at the beginning and the end of each pulse since the positive ion flux in an electronegative plasma is essentially described by  $n_i \cdot v_B = n_i \cdot \sqrt{k_B T_e \cdot (1 + \alpha_S) / m_i (1 + \alpha_S \eta)}$ , where  $\alpha_S = n_{i,-} / n_e$  is the ratio of negative ions to electrons and  $\eta = T_{e-} / T_{e+}$  is the ratio of negative ion temperature to electron temperature.<sup>31</sup> The slower increase during the on-time is mainly attributed to a change in ion density.

We also calculated the ion flux originating only from the on time, and the percentage it represents on the full ion flux.

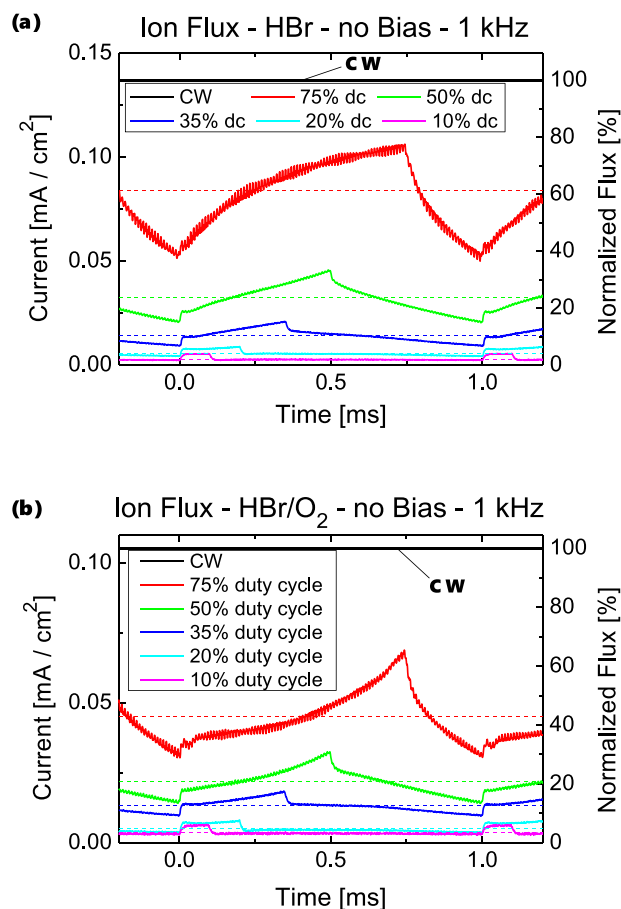


FIG. 5. (Color online) Ion flux from capacitive probe (IFP) measurements in pulsed (a) HBr and (b) HBr/O<sub>2</sub> plasmas at 20 mTorr, 750 W source power, and a frequency of 1 kHz. No bias power is applied.



The (mean) flux contribution from the on time is defined by  $\langle \Gamma_i \rangle_{on} = (1/T) \int_0^{dcT} \Gamma_i dt$  with  $dc$  the duty cycle,  $T$  the pulsing period and  $\Gamma_i$  the ion flux. The mean ion flux being defined as  $\langle \Gamma_i \rangle = (1/T) \int_0^T \Gamma_i dt$ , the percentage of the ion flux from the on time in comparison to the full ion flux is defined as  $\langle \Gamma_i \rangle_{on} / \langle \Gamma_i \rangle \cdot 100$ . The mean values for the ion fluxes and their relative contributions are given in Table I. They follow similar trends in both plasma conditions:

- (1) The mean flux increases approximately with the square of the duty cycle ( $dc^2$ ).
- (2) The percentage of the flux from only the on-time of the plasma (high energy ions) increases almost linearly with the duty cycle.

The second point is very important since it means that in a pulsed HBr/O<sub>2</sub> plasma, the relative amount of high energy (HE) ions can be drastically reduced. This might be a way to reduce surface damage from energetic ions.

By combining both observations, we can also state that in pulsed conditions, the ion flux from only the on-time of the plasma (i.e., the energetic ion dose) increases approximately with  $dc^3$  compared to CW mode.

#### IV. ION FLUX IN BIASED Si ETCH CONDITIONS

From theoretical considerations, the ion flux should not change much with different bias conditions since the plasma density is expected to be controlled mainly by the inductively coupled plasma source power which remains constant. However, changes in the plasma composition would lead to changes in the ion flux. With our plasma conditions, the silicon is not etched without bias power, while for bias powers larger than few tens of Watts, silicon is etched and the etch rate hardly varies with the bias power. Therefore, we expect a difference in plasma composition and therefore different ion fluxes without bias power and with bias power, when the plasma is fed with silicon etch by-products.

TABLE I. Measured (rounded) mean ion fluxes in HBr and HBr/O<sub>2</sub> plasmas at 20 mTorr, 750 W source power, and without bias at a pulse frequency of 1 kHz.

| Gas                | Duty cycle % | Mean flux $\mu A/cm^2$ | Mean flux % CW | Flux on-time % mean flux | Flux on-time % mean flux CW |
|--------------------|--------------|------------------------|----------------|--------------------------|-----------------------------|
| HBr                | 100          | 137                    | 100            | 100                      | 100                         |
|                    | 75           | 84                     | 61             | 79                       | 48                          |
|                    | 50           | 32                     | 24             | 54                       | 13                          |
|                    | 35           | 14                     | 10             | 41                       | 4.2                         |
|                    | 20           | 6                      | 4.1            | 28                       | 1.1                         |
|                    | 10           | 3                      | 2.0            | 18                       | 0.4                         |
| HBr/O <sub>2</sub> | 100          | 107                    | 100            | 100                      | 100                         |
|                    | 75           | 45                     | 42             | 76                       | 32                          |
|                    | 50           | 22                     | 20             | 54                       | 11                          |
|                    | 35           | 13                     | 13             | 40                       | 5.0                         |
|                    | 20           | 5                      | 4.6            | 29                       | 1.3                         |
|                    | 10           | 4                      | 3.3            | 16                       | 0.5                         |

#### A. CW plasma

Figure 6 shows the total ion flux with respect to the bias power for the HBr and HBr/O<sub>2</sub> plasma obtained from RFA and IFP measurements. Figure 7 shows the mean ion energy obtained in the same conditions with the RFA. While for the RFA measurements the ion flux of the pure HBr plasma is lower than the flux in the HBr/O<sub>2</sub> plasma, the opposite is the case for the IFP measurements. This difference is due to the different positions of the probes (the IFP is situated in plane with the reactor sidewall, the RFA lies on a dummy silicon wafer). Therefore, a direct comparison between both probes cannot be made.

##### 1. IFP results

The evolution of the ion flux with bias power from the IFP data shows a dependence on the used plasma chemistry. For the HBr case, the ion flux decreases slightly with higher bias power at first and starts to increase gradually afterwards. In the HBr/O<sub>2</sub> case, the flux is constantly increasing. At higher bias power both fluxes approach each other.

In both chemistries, the increase of the ion flux with the RF bias power is attributed mostly to the localized ionization produced by the capacitive coupling of the RF bias power to the chuck. This contribution to the total ionization rate in the plasma volume is small in high density plasma, but is nevertheless clearly captured by the ion flux probe for both plasmas and by the RFA probe for the HBr/O<sub>2</sub> plasma in Fig. 6.

It should also be underlined that the absolute value of the ion flux is small since it hardly reaches  $0.12 \text{ mA/cm}^2$ . This is attributed to the highly electronegative character of the HBr and HBr/O<sub>2</sub> plasmas.

##### 2. RFA results

Using the RFA, the ion flux and the ion energy can be determined and correlated. The dataset presented in Fig. 6 starts with a bias power of 20 W because the ceramic shield that we used to prevent the metallic body from being sputtered would induce a too large charging effect at lower bias power. Since it is dielectric, it might be charged differently compared to the wafer and the RFA body itself. For low ion energies, this difference might be sufficient to deflect ions and to reduce thereby the number of ions that reach the detector. Another possible reason is linked to the very thin plasma sheath in the case without bias. If the sheath is thin enough, the plasma might be able to extend to some degree into the holes of the dielectric shield.<sup>32</sup> Since the ion trajectory runs perpendicular to the sheath, the distortion in the proximity of the holes could deflect some ions toward the ceramic hole sidewalls so that they do not reach the RFA collector. Hence, we do not report the ion flux at 0 W bias here.

Comparing the RFA data for the ion flux and energy, two features can be observed: the total ion flux is increased when oxygen is added and at the same time, the mean ion energy is decreased. Furthermore, the ion energy increases linearly with the bias power. In a rough approximation, the bias power  $P_{\text{bias}}$  is proportional to the product of the ion flux  $\Gamma_i$  and the sheath voltage  $\bar{V}_s$  ( $\approx$  ion energy  $E_i$ )<sup>26</sup> if collisional

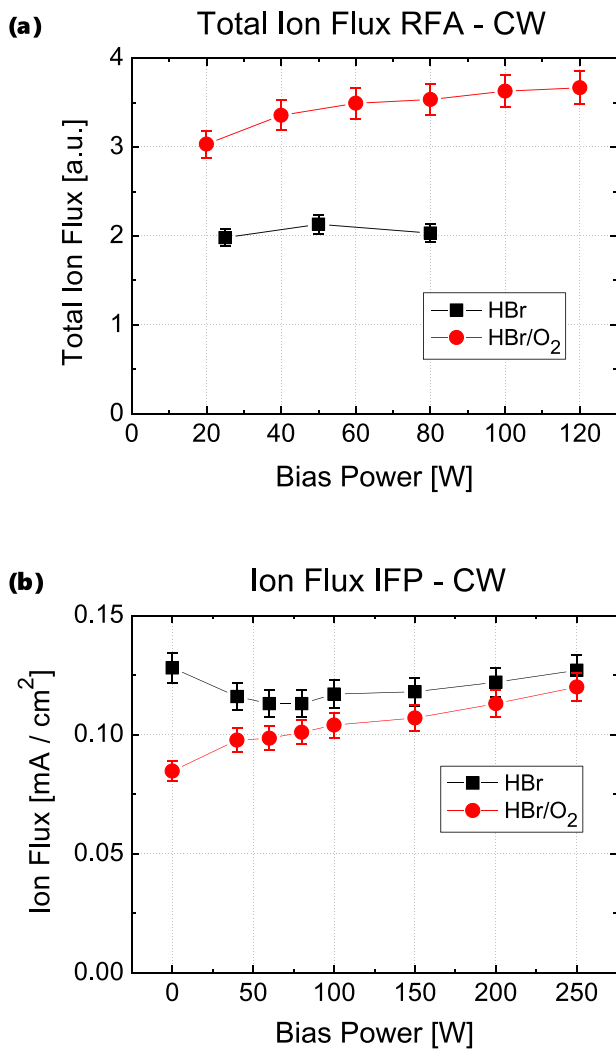


FIG. 6. (Color online) Total ion flux for different bias powers in CW mode at 20 mTorr and 750 W source power (HBr flow at 200 sccm and O<sub>2</sub> flow at 5 sccm): (a) RFA and (b) IFP data.

losses (e.g., ionization or charge transfer) and losses in the hardware (e.g., matchbox) are neglected. In other words, the applied bias power is mainly consumed by accelerating the ions. As discussed previously, this is a good approximation in our conditions since only little ionization is resulting from applying RF bias power to the wafer. In this case, the product of the ion flux and ion energy is proportional to the bias power. If the ion density and consequently also the ion flux increase while the bias power remains constant, the mean ion energy decreases.<sup>26</sup> In the case of added oxygen, the total ion flux is increased according to the RFA measurements. Hence, the mean ion energy of the IVDF should decrease (as observed).

Furthermore, in both plasma chemistries, the ion flux is almost constant with changing bias power. Hence, an increase in bias power leads to the linear increase in mean ion energy, as observed in Fig. 7.

Since the voltages applied to the RFA are limited to a maximum of 400 V, the IVDF for the process plasma with 200 W bias power could not be measured. Based on the linear approximation of the ion energy, we can estimate for this

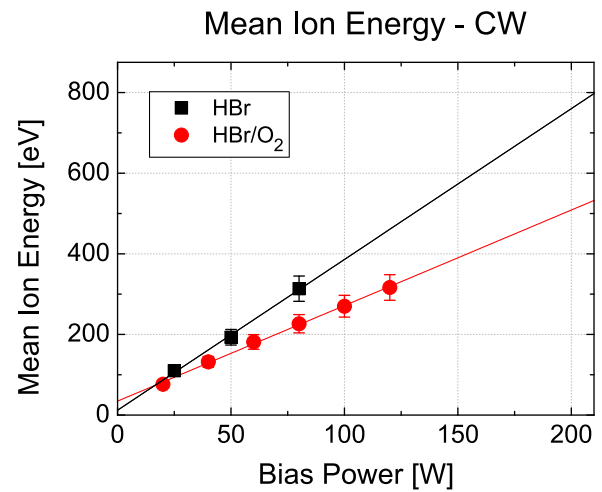


FIG. 7. (Color online) RFA measurements of the mean ion energy in CW at 20 mTorr and 750 W source power.

case a mean energy of approximately 500 and 750 eV for the HBr/O<sub>2</sub> and the HBr plasma, respectively. These energies are high for an ICP plasma, but they are a direct consequence of the low value of the ion current in HBr-based plasmas.

## B. Pulsed plasma

As shown in Sec. III for the case without bias power, the ion flux decreases with lower duty cycle since the ion density in the plasma is reduced. This evolution is unchanged if pulsed bias power is applied synchronously with the source power. During the on-time of the plasma, the instantaneous bias power is the same as for CW, but the ion flux is significantly lower, which leads to a much higher ion energy in pulsed mode.

Figure 8 shows the time averaged IVDF for a pulsed HBr plasma at different duty cycles, as well as the corresponding ion flux. The plasma conditions studied here (10 mTorr, 1200 W source power, 60 W bias power) are significantly different from the standard etch process studied previously: the ICP power was increased to obtain a signal which is strong enough to be analyzed while the bias power was reduced to be able to measure the ion energy (our sensor stops at 400 eV). Also, a different dielectric shield for the RFA was used (anodized probe body instead of additional ceramic shield).

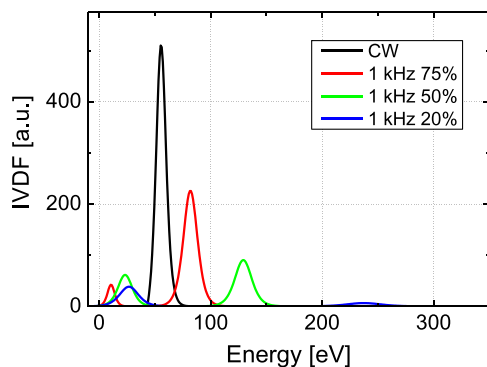
In CW mode, a single peak IVDF is measured. If the plasma is pulsed, a low energy (LE) peak from the afterglow appears in addition to the HE peak from the active source and bias power period. For the low energy peak, we would expect an energy of just a few eV, corresponding to a vanishing sheath voltage in the afterglow. The rather high measured energy and its slow evolution might be linked to the poor measurement accuracy for the RFA floating potential that is used to calibrate the IVDF and/or to an imperfect filtering at 1 kHz. Also, for low energy ions, charge effects that derogate the IVDF measurement might play a role, as discussed for the ion flux measurement in CW conditions without bias power. Therefore, the energy value from the LE peak will not be discussed. Nevertheless, the measured ion

flux of both peaks and the very large energy shift for the HE peak are assumed to be correct.

For decreasing duty cycles, the high energy peak shifts to very large values due to the decreasing ion flux. The ratio between high and low energy flux is decreasing until the high energy flux becomes almost insignificant, shown in Fig. 8(b). This is in good agreement with the time-resolved measurement of the ion flux in no-bias conditions in Sec. III and might open the possibility to reduce surface damage caused by high energy ions. It is important to underline that although the high energy flux is strongly reduced, for a given RF biasing power the ion energy of this flux is multiplied by more or less a factor of 5 when the plasma is pulsed at 20% duty cycle. It follows that when the plasma is pulsed under our typical etching conditions at this duty cycle (with 750 W source and 200 W bias), the ion energy is estimated to be about 2.5 keV, leading to very specific etching conditions compared to what can be obtained in a CW plasma. Indeed, since the wafer is bombarded by a low flux of very energetic ions, we are in a condition that resembles those obtained in purely capacitively coupled reactors, but at lower pressure with collisionless sheaths and with a high flux of low energy ions during the off-time of the plasma pulses.

With increasing the pulsing frequency the IVDF also changes, but only slightly. Unfortunately, the ion current measurement data are very noisy for high frequencies, and hence,

(a) IVDF from HBr Plasma at 1 kHz Pulsing



(b) Ion Flux and Energy vs. CW Mode

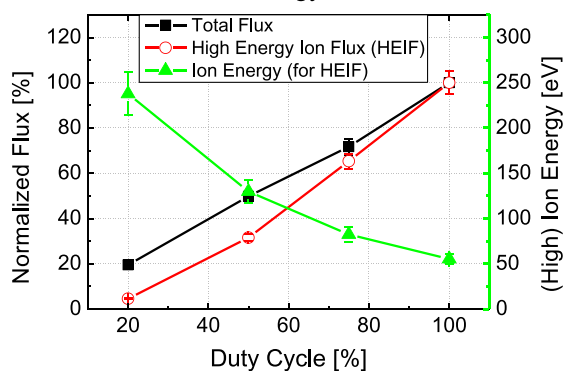


FIG. 8. (Color online) (a) IVDFs of a pulsed HBr plasma (200 sccm, 10 mTorr, 1200 W source power, 60 W bias power) at 1 kHz with bias. (b) Corresponding total ion flux, high energy ion flux and mean energy of the latter.

it is difficult to derive a meaningful IVDF from it. However, it is quite straightforward to extract the total ion flux, which is shown in Fig. 9 for several duty cycles and frequencies.

For all duty cycles, the total ion flux decreases if the frequency is increased, comparable to a further reduction of the duty cycle. The relative reduction of the ion flux becomes stronger for lower duty cycle. At higher frequencies, the number of transitions per second between on and off increases and the pulse period could become so small that it approaches the characteristic time constants for ionization, dissociation, and recombination, even more at low duty cycles.

Furthermore, even if our system is working at constant absorbed power (the reflected power is measured and compensated), it is difficult to determine how much of this power is really absorbed by the plasma species and how much is dissipated in the matching units. In other words, since matching the plasma impedance becomes more and more difficult as the pulsing frequency is increased, it is possible that a slightly lower RF power is delivered to the plasma at high frequency, thus participating to a reduction of the ion flux.

## V. SUMMARY

In the first part of the article, the ion flux was studied in an HBr/O<sub>2</sub> plasma without applied bias power.

Depending on the nature of the reactor wall and the gas composition of the plasma, the ion flux varies significantly. This is due to the changed reaction coefficients on the chamber walls that affect the plasma composition and therefore the ion flux.

When the plasma is pulsed, the time variations of the ion flux during the pulse depend also on the plasma chemistry: while the flux rises strongly at first and then slows down in a pure HBr plasma, the opposite is observed for the HBr/O<sub>2</sub> plasma.

By reducing the duty cycle, the average ion flux decreases by approximately the square of the duty cycle ( $dc^2$ ) and the percentage of the ion flux that originates from the on-time of the plasma almost linearly. Hence, the average ion flux from only the on-time of the plasma decreases by roughly  $dc^3$

HBr - Total Ion Flux

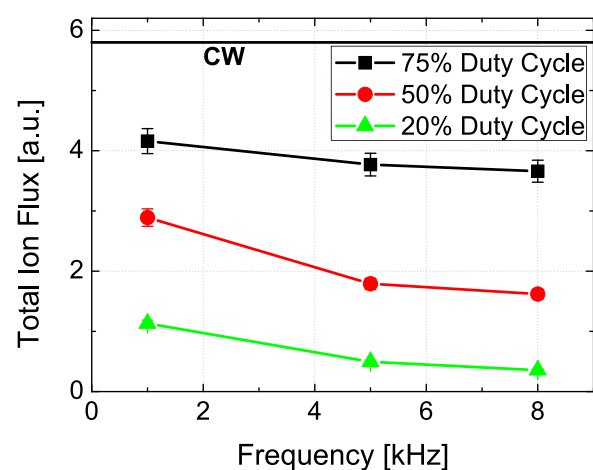


FIG. 9. (Color online) Ion flux for pulsed HBr plasmas (200 sccm, 10 mTorr, 1200 W source power, and 60 W bias power) from RFA measurements.



compared to the CW case. The reduction of the relative contribution of high energy ions to the total flux might be useful to reduce damages from energetic ions although their ion energy itself increases.

In the second part of the article, the ion flux was investigated in silicon etch conditions with applied bias power (200 W). The results indicate mean ion energies of approximately 500 and 750 eV for the CW HBr/O<sub>2</sub> and the CW HBr plasma, respectively.

The total ion flux increases slightly with higher bias power due to an increase of the density of silicon etch product in the gas phase as well as to a non-negligible local ionization in front of the sheath that is facing the RF biased wafer. Directly on the wafer, the ion flux from an HBr/O<sub>2</sub> plasma is higher than in the pure HBr chemistry. The opposite is observed with the IFP at the reactor sidewall. The reason for this difference is not fully understood but attributed to spatial density gradients of the charged species in the reactor.

For pulsed mode, the IVDF shows a high and a low energy peak, which correspond to the ions from the on- and the off-time of the plasma, respectively. If the duty cycle is reduced, the total ion flux, measured by the RFA on the wafer, decreases linearly and the high energy peak shifts to even higher energies. The relative contribution from the high energy peak to the total ion flux is also reduced with the duty cycle, leading to an overall decreased averaged ion energy. These results are in good agreement with the IFP measurements in unbiased conditions.

Similar to a decrease in duty cycle, also an increase in frequency, especially for low duty cycles, results in a further reduction of the total ion flux.

## ACKNOWLEDGMENT

This work was partly supported by the French RENATECH network.

<sup>1</sup>T.-H. Ahn, K. Nakamura, and H. Sugai, *Plasma Sources Sci. Technol.* **5**, 139 (1996).

<sup>2</sup>G. S. Hwang and K. P. Giapis, *Jpn. J. Appl. Phys.* **37**, 2291 (1998).

<sup>3</sup>J.-H. Kim, C.-J. Kang, T.-H. Ahn, and J.-T. Moon, *Thin Solid Films* **345**, 124 (1999).

<sup>4</sup>S. Samukawa and K. Terada, *J. Vac. Sci. Technol.*, **B 12**, 3300 (1994).

<sup>5</sup>S. Samukawa, K. Noguchi, J. I. Colonell, K. H. A. Bogart, M. V. Malyshev, and V. M. Donnelly, *J. Vac. Sci. Technol.*, **B 18**, 834 (2000).

<sup>6</sup>S. Samukawa and T. Mieno, *Plasma Sources Sci. Technol.* **5**, 132 (1996).

<sup>7</sup>C. Petit-Etienne, M. Darnon, L. Vallier, E. Pargon, G. Cunge, F. Boulard, O. Joubert, S. Banna, and T. Lill, *J. Vac. Sci. Technol.*, **B 28**, 926 (2010).

<sup>8</sup>C. Petit-Etienne, E. Pargon, S. David, M. Darnon, L. Vallier, O. Joubert, and S. Banna, *J. Vac. Sci. Technol.*, **B 30**, 40604 (2012).

<sup>9</sup>S. A. Voronin, M. R. Alexander, and J. W. Bradley, *Meas. Sci. Technol.* **16**, 2446 (2005).

<sup>10</sup>H. Ohtake, K. Noguchi, S. Samukawa, H. Iida, A. Sato, and X. Qian, *J. Vac. Sci. Technol.*, **B 18**, 2495 (2000).

<sup>11</sup>S. Samukawa, Y. Ishikawa, S. Kumagai, and M. Okigawa, *Jpn. J. Appl. Phys.* **40**, L1346 (2001).

<sup>12</sup>M. Okigawa, Y. Ishikawa, and S. Samukawa, *Jpn. J. Appl. Phys.* **42**, 2444 (2003).

<sup>13</sup>P. Subramonium and M. J. Kushner, *J. Appl. Phys.* **96**, 82 (2004).

<sup>14</sup>G. Cunge, D. Vempaire, and N. Sadeghi, *Appl. Phys. Lett.* **96**, 131501 (2010).

<sup>15</sup>R. W. Boswell and D. Henry, *Appl. Phys. Lett.* **47**, 1095 (1985).

<sup>16</sup>N. St. J. Braithwaite, J. P. Booth, and G. Cunge, *Plasma Sources Sci. Technol.* **5**, 677 (1996).

<sup>17</sup>J. P. Booth, N. St. J. Braithwaite, A. Goodyear, and P. Barroy, *Rev. Sci. Instrum.* **71**, 2722 (2000).

<sup>18</sup>D. Gahan, B. Dolinaj, and M. B. Hopkins, *Rev. Sci. Instrum.* **79**, 033502 (2008).

<sup>19</sup>D. Gahan, S. Daniels, C. Hayden, D. O'Sullivan, and M. B. Hopkins, *Plasma Sources Sci. Technol.* **21**, 015002 (2012).

<sup>20</sup>M. Haass, M. Darnon, G. Cunge, and O. Joubert, *J. Vac. Sci. Technol.*, **B 33**, 032203 (2015).

<sup>21</sup>E. Pargon, O. Joubert, T. Chevolleau, G. Cunge, S. Xu, and T. Lill, *J. Vac. Sci. Technol.*, **B 23**, 103 (2005).

<sup>22</sup>G. Cunge, R. L. Inglebert, O. Joubert, L. Vallier, and N. Sadeghi, *J. Vac. Sci. Technol.*, **B 20**, 2137 (2002).

<sup>23</sup>P. Bodart, M. Brihoum, G. Cunge, O. Joubert, and N. Sadeghi, *J. Appl. Phys.* **110**, 113302 (2011).

<sup>24</sup>S. Banna *et al.*, *IEEE Trans. Plasma Sci.* **37**, 1730 (2009).

<sup>25</sup>M. Darnon, G. Cunge, and N. St. J. Braithwaite, *Plasma Sources Sci. Technol.* **23**, 025002 (2014).

<sup>26</sup>M. Brihoum, G. Cunge, M. Darnon, D. Gahan, O. Joubert, and N. St. J. Braithwaite, *J. Vac. Sci. Technol.*, **A 31**, 020604 (2013).

<sup>27</sup>G. Cunge, M. Kogelschatz, and N. Sadeghi, *Plasma Sources Sci. Technol.* **13**, 522 (2004).

<sup>28</sup>G. Cunge, M. Kogelschatz, O. Joubert, and N. Sadeghi, *Plasma Sources Sci. Technol.* **14**, S42 (2005).

<sup>29</sup>G. Cunge, N. Sadeghi, and R. Ramos, *J. Appl. Phys.* **102**, 093305 (2007).

<sup>30</sup>G. Cunge, D. Vempaire, R. Ramos, M. Touzeau, O. Joubert, P. Bodard, and N. Sadeghi, *Plasma Sources Sci. Technol.* **19**, 034017 (2010).

<sup>31</sup>M. A. Lieberman and A. J. Lichtenberg, *Principles of Plasma Discharges and Materials Processing* (Wiley-Interscience, New York, 1994).

<sup>32</sup>C. Böhm and J. Perrin, *Rev. Sci. Instrum.* **64**, 31 (1993).